PAPER

Check for updates

Armchair shaped polymeric nitrogen N_8 chains confined in h-BN matrix at ambient conditions: stability and vibration analysis†

Shuang Liu,[a] Bo Liu,[a] Zhen Yao,[a] Shijie Liu, [iD][b] Xuhan Shi,[a] Shifeng Niu[a] and Bingbing Liu [iD] *[a]

A new hybrid material comprising of armchair shaped polymeric nitrogen chains (N_8) encapsulated in h-BN matrix is proposed and studied through *ab initio* calculations. Interestingly, the theoretical results demonstrate that N_8 chains, confined in h-BN matrix, are effectively stabilized at ambient pressure and room temperature. Moreover, N_8 chains can dissociate and release energy at a much milder temperature of 600 K. The confined polymer N_8 unit needs to absorb 0.68 eV energy to span the decomposition energy barrier before decomposing. Further research shows that the charge transfer between N_8 chain and h-BN layer is the stabilizing mechanism of this new hybrid material. And the low dissociation temperature is due to a much smaller amount of charge transfer compared to other confined systems in previous reports. The IR and Raman vibrational analyses suggest that host–guest interactions in the hybrid material influence the vibration modes of both the confined N_8 chain and h-BN layer.

1 Introduction

Polymeric nitrogen, a typical high-energy-density material (HEDM), is a potential candidate in several applications such as explosives, propellants and energy storage.[1–3] Due to the large energy difference between the single bond and the triple bond, a large amount of energy is released during the transformation of nitrogen phase from single-bonded state to molecular state.[4,5] More importantly, nitrogen gas, the decomposition product of polymeric nitrogen, is environmentally friendly.[5,6] Over the years, remarkable progress has been made towards the design and synthesis of polymeric nitrogen.[7–10] In theoretical calculations, many novel forms of polymeric nitrogen have been proposed under high pressure, including purely single-bonded structures,[1,6,9,11–14] chain structures containing alternating single and double bonds,[15] and the molecular solids.[8,16] In experiments, the single-bonded network form of polymeric nitrogen (cg-N) was synthesized at 110 GPa and 2000 K for the first time. In 2014, a layered polymeric nitrogen (LP-N) has also been obtained under much harsher conditions (150 GPa, 3000 K) using laser-heated diamond anvil cells.[5] Lately, a hexagonal layered polymeric nitrogen phase (HLP-N) was prepared near

250 GPa by compressing and laser heating pure nitrogen.[7] Unfortunately, these obtained polymeric nitrogen are unstable at ambient conditions. Thus, an effective strategy is needed to stabilize polymeric nitrogen at ambient pressure and room temperature.

Recently, a new hybrid material comprising of polymeric nitrogen chains (N_8) with armchair shape encapsulated in the confined space has gathered significant interest. Theoretical studies indicate that N_8 chains could be effectively stabilized at ambient conditions by being confined in 1-D space of nano-tubes or 2-D space of a graphene matrix.[17–21] Further analysis shows that the charge transfer from the host materials to N_8 chains is the major reason for the stability of guest material.[17,19] In experiment, N_8^- molecular anion is stabilized at ambient conditions on the positively charged sidewalls of multi-walled carbon nanotubes (MWNTs).[22] Several theoretical researches have revealed that nano-confinement is an effective strategy for stabilizing polymeric nitrogen at ambient conditions.[17,19–21] The MD studies indicate that the strong host–guest interaction in these hybrid structures results in a dissociation temperature of N_8 chains higher than 1400 K, and over 5000 K.[17,19] This is the drawback that limits their applications. Thus, it is urgent to explore an ideal host material for both stabilizing N_8 chain at ambient conditions and allowing its energy releasing under controllable conditions.

Boron nitride (BN) matrix, analogous to graphene matrix, is commonly used in pollutant adsorption, catalysis and especially in protective capsules for holding materials under extreme conditions due to its superb heat resistance, low density, admirable temperature stability, chemical durability and

[a] State Key Laboratory of Superhard Materials, Jilin University, Changchun 130012, P. R. China. E-mail: liubb@jlu.edu.cn

[b] School of Physics and Engineering, Henan Key Laboratory of Photoelectric Energy Storage Materials and Applications, Henan University of Science and Technology, Luoyang, 471003, P. R. China

oxidizing properties.[23–27] However, BN matrix has not been investigated as a host material to confine polymeric nitrogen chains.

In this work, a multilayer h-BN matrix is proposed as a host material to confine the polymeric N_8 chains, forming a new hybrid material (N_8@h-BN matrix). The research focuses on three goals: investigating the stability of confined polymeric N_8 chains; obtaining a further understanding of its stability mechanism; exploring the influence of systematic interactions on the vibration optic modes of host and guest materials.

2 Model and computational method

Two comparative calculations are performed to confirm the optimal structure and arrangement of confined N_8 chain inside h-BN matrix. Firstly, we performed the geometry optimization for both the zigzag and armchair N_8@h-BN crystal structures (see Fig. S1†). The results show that the zigzag N_8 chain relaxed into the twisty armchair N_8 chain, indicating that the confined zigzag N_8 chain is unstable. For comparison, the energy (−268.87 eV) of armchair N_8@h-BN structure is smaller than that (−268.82 eV) of twisty armchair N_8@h-BN structure, which means that the confined armchair N_8 chain is energetic stability. Secondly, in order to obtain the optimal arrangement of N_8@h-BN structure, the $1 \times 2 \times 2$ supercell structure of h-BN matrix with the different molecular orientation of N_8 is constructed. The DFT total energy calculation shows that the hybrid N_8@h-BN structure with the laying N_8 molecule in the *oc* direction is the optimal structure (Fig. S2†). As shown in Fig. 1, a triclinic periodic unit model is built for the theoretical study with lattice constants of *oa*, *ob* and *oc* being 8.72, 8.68 and 7.6 Å, respectively. The angles *aob*, *aoc* and *boc* are 105°, 90° and 90°, respectively. The h-BN matrix and armchair-shape N_8 chain are parallel to each other on the *obc* plane and N_8 chain extends along the *oc* direction. The lattice mismatch is 0.0435 (see ESI†) and it allowed to keep the system size at computationally affordable level. The length of alternating single and double bonds of N_8 chain are 1.30 and 1.29 Å, respectively, which is in agreement with the reported values of 1.34 Å and 1.29 Å.[19] The initial distance of h-BN matrix and N_8 chain is about 3.5 Å.
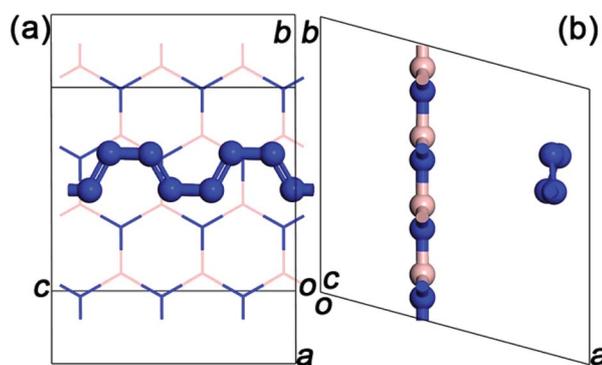
Calculations of the geometry relaxation and the electronic properties are performed within the unit cell model. Molecular dynamic (MD) simulations are performed within the $2 \times 1 \times 1$ supercell model. The Vienna *ab initio* simulation package (VASP), which is based on the density functional theory (DFT), is applied in the calculation.[28,29] The exchange–correlation interaction is described by the generalized gradient approximation (GGA).[30] The plane-wave energy cutoff is taken as 520 eV. For Brillouin zone integrations, $5 \times 5 \times 5$, $9 \times 9 \times 9$ and $1 \times 1 \times 1$ Monkhors Pack grid are used for the structural relaxation, electronic properties and MD simulation, respectively. The convergence criterion of force and energy are 0.05 eV per atom and 10^{-6} eV, respectively. For the MD simulation, the total simulation time is 10 ps, and the time step is $\Delta t = 1 \times 10^{-3}$ ps. The temperature of simulated system is controlled by the Nose thermostat. We performed the MD simulation at constant number of molecules *N*, constant volume *V* and constant temperature *T*, representing a canonical or *NVT*-ensemble.

3 Results and discussion

The stability analysis of confined polymeric N_8 chain is performed by the MD simulation. Seven temperatures (100–700 K) are considered for the simulation of *NVT*-ensemble. In Fig. 2(a), we extract the last 2 ps from the 10 ps. The bond lengths of single and double bonds in N_8 chain are recorded as the MD time at different temperatures. As the MD time progresses, lengths of single and double bonds are found to oscillate irregularly in the range of 1.29–1.39 Å and 1.21–1.30 Å, respectively. Meanwhile, the average length of single and double bonds as a function of simulated temperatures is shown in Fig. 2(b). To visualize our analysis, four MD simulated N_8@h-BN matrix structures are presented in Fig. 3. As the temperature increases, the average length of single bond increases linearly with a slope of 2.39×10^{-5}, whereas a decreasing trend is observed for the double bond with a slope of -8.03×10^{-7}. For comparison, length of single bond length exhibits a much larger varying rate. The increasing and decreasing tendency of single and double bonds suggest that the N_8 chain gradually loses its uniform chain properties with the increased temperature, but also keeps its chain configuration up to 500 K (Fig. 3(a) and (b)). At a temperature of 600 K, one bond length (1.125 Å) is obtained, indicating that the chain structure begins to decompose and transforms to the N_2 molecular phase (see Fig. 3(c)). A much larger decompose rate is evident at a temperature of 700 K (see Fig. 3(d)). These results suggest that the confined N_8 chain inside h-BN matrix is stable at ambient conditions and maintains its configuration up to 500 K. The decomposition temperature is 600 K, which is lower than that of N_8 chain being confined inside the 1-D BN nanotube (1400 K)[19] and much lower than that of N_8 chain being confined inside 1-D carbon nanotube (5000 K).[17] Thus, the h-BN matrix can be an excellent confinement material for polymeric N_8 chain, due to the mild and controllable energy releasing temperature of N_8 chain as well as the high stability of host molecule.

Furthermore, the decomposition energy and the corresponding energy barrier are calculated to further confirm the
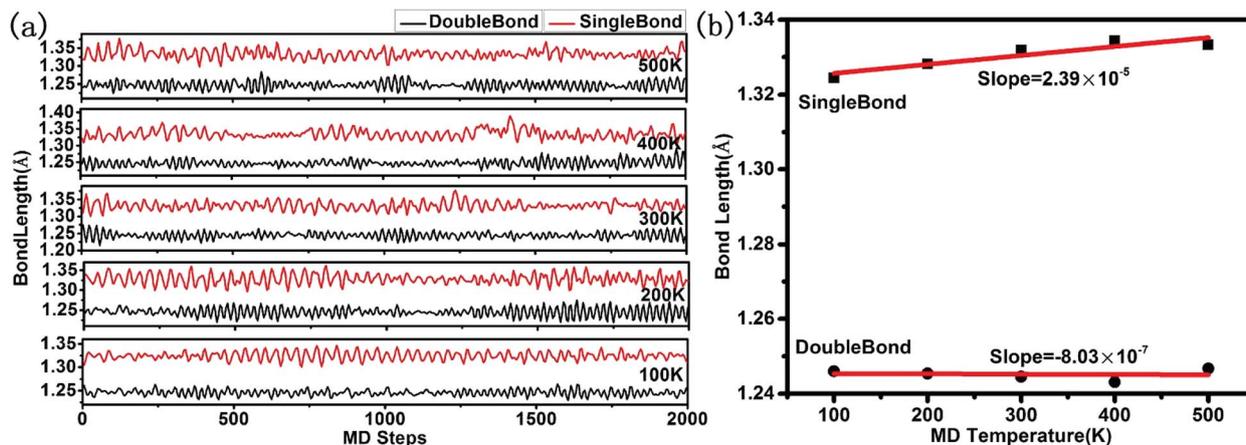

Fig. 1 (a) Unit cell of N_8@h-BN crystal structure. (b) View in the oab plane.

Fig. 2 (a) The evolution of single and double bond length of N_8 chain with the MD time at different temperatures. (b) The average of single and double bond length as the function of the simulated temperatures.
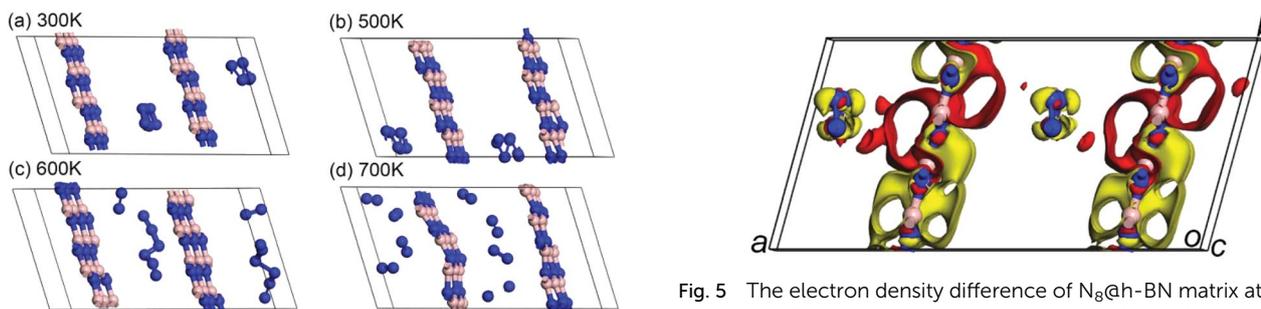

Fig. 3 Snapshots of N_8@h-BN matrix structure at 300 K (a), 500 K (b), 600 K (c) and 700 K (d).

Fig. 5 The electron density difference of N_8@h-BN matrix at ambient conditions. Red and yellow colours represent effective positive and negative charges, respectively.

stability of encapsulated N_8 chain in h-BN matrix. We extract the confined N_8 chain, $N_2 + N_6$ and $4N_2$ structures and performed the DFT total energy calculation. As shown in Fig. 4, the left N_8 chain with the energy of -57.96 eV is the full relaxed structure; while the right one with the energy of -57.28 eV is the structure before decomposing in MD simulation. The energies of intermediate structure ($N_2 + N_6$ in MD simulation) and the

decomposed structure ($4N_2$ after the relaxation) are -60.65 eV and -65.13 eV, respectively. The decomposition energy barrier (0.68 eV) is just the energy difference ($\Delta E = 57.96-57.28$) of two N_8 structures; while the decompose energy of one N_8 unit (7.17 eV) is the energy difference ($\Delta E = 65.13-57.96$) of two relaxed structures. Thus, the confined polymer N_8 unit needs to absorb 0.68 eV energy to span the decomposition energy barrier before
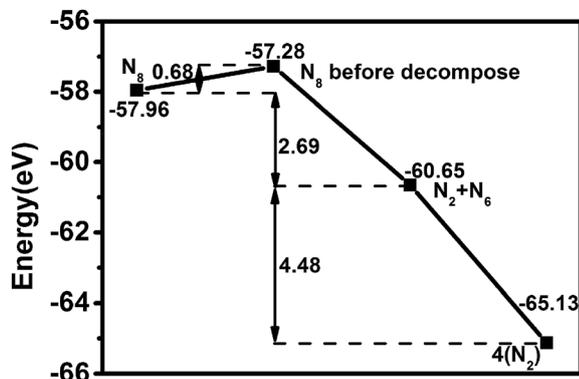

Fig. 4 Energy of N_8 with full relaxed, the N_8 before decompose in MD simulation, $N_2 + N_6$ in MD simulation, $4N_2$ with full relaxed.
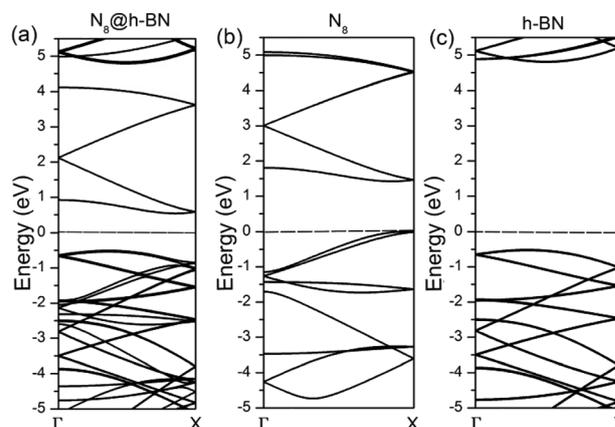

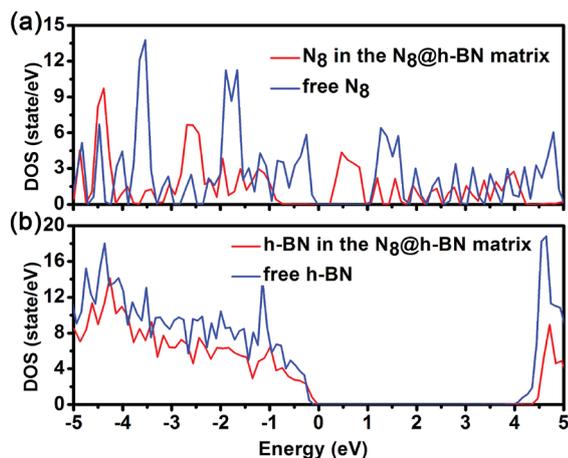**Fig. 6** Band structures of N_8@h-BN system (a), isolated N_8 chain (b) and isolated h-BN layer (c).

Fig. 7 Density of states for free h-BN layer and h-BN layer in the N_8@h-BN system (a) and density of states for the free N_8 chain and N_8 chain in the N_8@h-BN system (b).

decomposing, which confirms its dynamical stability at ambient conditions. After spanning the energy barrier, one polymer N_8 unit releases 7.17 eV when it decomposed into $4N_2$ molecules.

For the second goal: obtaining a further understanding of stable mechanism. As previous reports, the charge transfer between the guest and the host materials is responsible for the stability of guest material.[17] Thus, the stability and much lower decomposition temperature of confined N_8 chain inside h-BN matrix should be induced by the different charge transfer. The electronic density difference of N_8@h-BN matrix, which is the total electronic density minus the electronic density of isolated h-BN matrix and N_8 chain, is shown in Fig. 5. Increased negative charges can be seen around the N_8 chain indicating the capture of electrons; while increased positive charges near the h-BN matrix suggests losing of electrons. Charge transfer mainly occurs between the N_8 chain and the nitrogen atoms in h-BN matrix, due to the polar B–N bonds since most of electrons are located near nitrogen atoms. Bader charge transfer analysis shows that each nitrogen atom of N_8 chain captures 0.004e from

the h-BN layer, which is smaller than the N_8@CNTs[17] (0.05e per atom) and N_8@BNNTs[19] (0.04e per atom) systems. Thus, it can be concluded that the charge transfer between host and guest molecule tends to stabilize the confined N_8 chain. More importantly, the stability of confined guest material is sensitive to the quantity of electrons transfer. This indicates that the more or less quantities of electrons transferring are corresponds to the more or little stable guest moleculer respectively. Compared to N_8@CNTs[17] and N_8@BNNTs[19] systems, the N_8@h-BN matrix transfers fewer number of electrons, which not only stabilizes the confined N_8 chain at ambient conditions, but also favors its application due to the much lower decomposition temperature.

To deeply understand the interaction between h-BN layer and N_8 chain, the band structure and density of states (DOS) of N_8@h-BN system are calculated, as shown in Fig. 6 and 7, respectively. The band structure and DOS of isolated N_8 chain and h-BN matrix are also calculated for comparative analysis. It is evident that the band structure of N_8@h-BN matrix is nearly the simple superposition of the individual band structures of isolated N_8 chain and h-BN matrix. The conduction band of N_8 chain in the system exhibits a downward shift compared to that isolated case, which is consistent with the fact that the charge transfer occurs from h-BN matrix to N_8 chain. Moreover, this charge transfer also induces a decrease of band gap of N_8@h-BN matrix. As shown in Fig. 7, the DOS curves of isolated h-BN matrix and N_8 chain are similar to that of N_8@h-BN matrix, while the energy of DOS peaks of N_8 chain exhibits a downshift compared to the isolated N_8 chain, which is also consistent with above analysis that the charge transfer occurs from h-BN matrix to N_8 chain. Thus, the band structure and DOS analysis further corroborate the electronic density difference analysis suggesting that the charge transfer is the mainly responsible for the stability of confined N_8 chain inside h-BN matrix.

For the third goal: exploring the influence of the systemic interaction on the vibration optic modes of host and guest materials. Calculated IR and Raman spectrum of isolated h-BN, isolated N_8 chain and N_8@h-BN matrix are shown in Fig. 8(a) and (b), respectively. Vibration modes are shown in Fig. 9 and

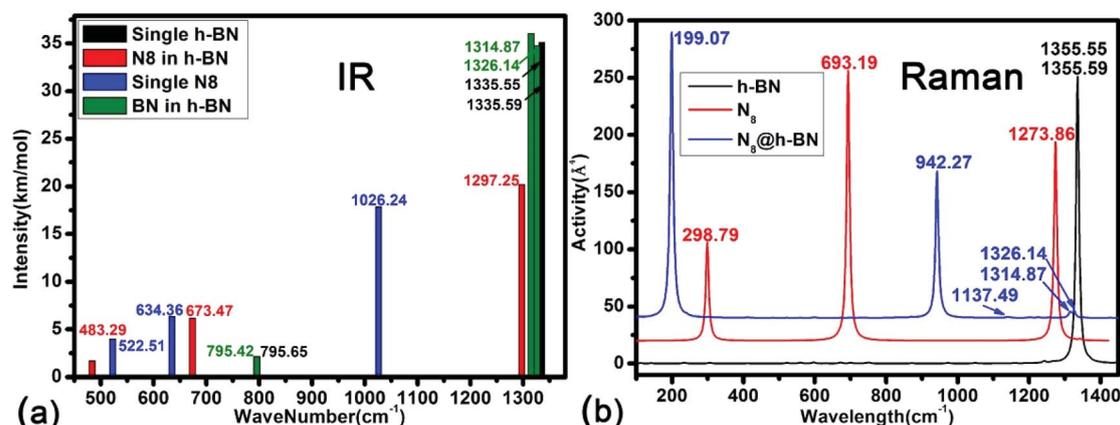**Fig. 8** Calculated IR and Raman spectrum of isolated h-BN, isolated N_8 chain and N_8@h-BN matrix are presented in (a) and (b).
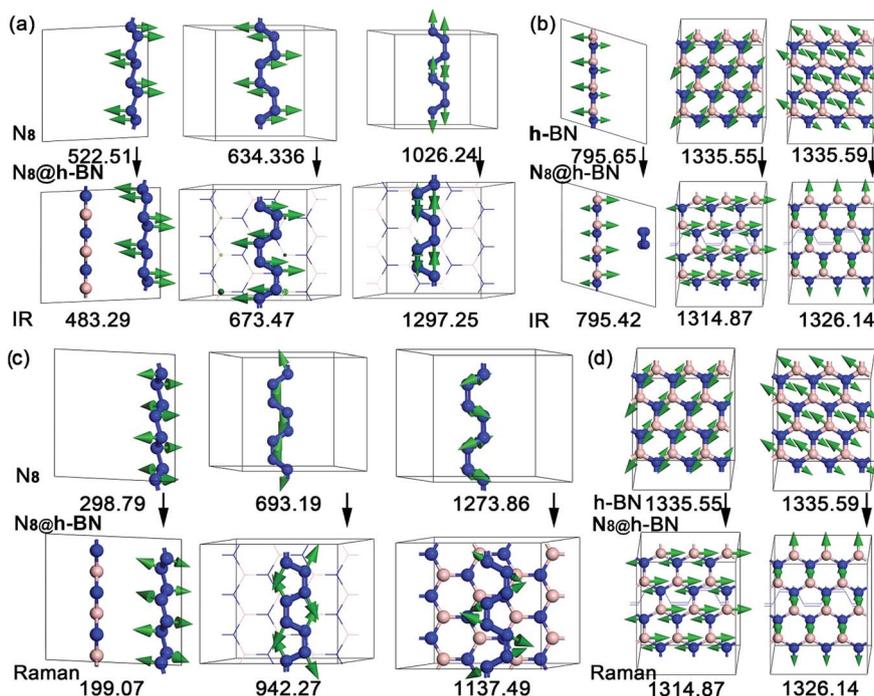
Fig. 9 Vibration modes of IR and Raman spectrums of isolated h-BN, isolated N_8 chain and N_8@h-BN matrix.

the corresponding vibration mode assignments are listed in Table 1. From the IR spectrum shown in Fig. 8(a), it is evident that N_8 chain and h-BN matrix exhibit three vibration models. For the N_8 chain, the host–guest interaction induces a blue shift and two red shift vibrations, which correspond to the blue shift of N_2–N_2–N_2 bending vibration (522.51 cm^{-1} → 483.29 cm^{-1}), the red shift of N_2–N_2–N_2 bending vibration (634.36 cm^{-1} → 673.47 cm^{-1}) and N–N stretch vibration (1026 cm^{-1} → 1297.25 cm^{-1}), respectively (see Fig. 9(a)). For the h-BN matrix, the host–guest interaction induces a blue shift of three vibration modes, which correspond to the B–N–B bending vibration (795.65 cm^{-1} → 795.42 cm^{-1}), the B–N stretch vibrations of (1335.55 cm^{-1} → 1314.87 cm^{-1}) and (1335.59 cm^{-1} → 1326.14 cm^{-1}) (see Fig. 9(b)). For the Raman spectrum shown in Fig. 8(b), it can be seen that the N_8 chain and h-BN exhibit three and two vibration modes, respectively. As induced by the host–guest interaction, two blue shifts (298.79 cm^{-1} → 199.07 cm^{-1}), (1273.86 cm^{-1} → 1137.49 cm^{-1}) and one red shift (693.19 cm^{-1} → 942.27 cm^{-1}) are observed for the N–N–N bending vibrations of N_8 chain (see Fig. 9(c)). Since the B–N–B bending and B–N stretch vibrations can be detected by both the IR and Raman spectrum, the same blue shift of B–N–B bending vibration (1335.55 cm^{-1} → 1314.8 cm^{-1}) and B–N stretch vibration (1335.59 cm^{-1} → 1326.14 cm^{-1}) are evident in the IR spectrum (see Fig. 9(d)). For the N_8 chain, the vibrations (522.51 cm^{-1} → 483.29 cm^{-1}, 298.79 cm^{-1} → 199.07 cm^{-1}, 1273.86 cm^{-1} → 1137.49 cm^{-1}), which are mainly perpendicular to the h-BN layer plane, exhibit a blue shift due to the confinement effect that suppresses these vibrations. The vibrations (634.36 cm^{-1} → 673.47 cm^{-1}, 1026 cm^{-1} → 1297.25 cm^{-1}, 693.19 cm^{-1} → 942.27 cm^{-1}) which are mainly parallel to the h-BN layer plane,

exhibit a red shift due to the much smaller confinement effect along this direction. All the vibrations of filled h-BN layer are blue shift compared with the single h-BN layer due to the host–guest interaction. The exhibited blue shift of vibration modes indicates a decreased vibration energy of h-BN layer, which is consistent with our electronic analysis that indicated a loss of electrons for the h-BN layer. Thus, the weak host–guest

Table 1 Vibration modes of IR and Raman spectra along with their assignments

	Symmetry	Assignment	N_8	N_8@h-BN
IR	—	N_2–N_2–N_2 bend	522.51	483.29
	—	N_2–N_2–N_2 bend	634.36	673.47
	—	N–N stretch	1026.24	1297.25

	Symmetry	Assignment	h-BN	N_8@h-BN
IR	A_{2u}	B–N–B bend	795.65	795.42
	E_{2g}	B–N–B bend	1335.55	1314.87
	E_{1u}	B–N stretch	1335.59	1326.14

	Symmetry	Assignment	N_8	N_8@h-BN
Raman	—	N–N–N bend	298.79	199.07
	—	N–N–N bend	693.19	942.27
	—	N–N–N bend	1273.86	1137.49

	Symmetry	Assignment	h-BN	N_8@h-BN
Raman	E_{2g}	B–N–B bend	1335.55	1314.87
	E_{1u}	B–N stretch	1335.59	1326.14

interaction also induces a red or blue shift of both the confined N_8 chain and h-BN matrix by the IR and Raman vibration analyses. This vibration analysis as well as the modes assignment can be used to guide the further studies in experiment.

4 Conclusions

In summary, we proposed a new hybrid structure, comprising of polymeric nitrogen chains (N_8) confined in a multilayer h-BN matrix and investigated its properties using *ab initio* DFT calculations. MD simulation results show that the polymeric nitrogen chains confined in h-BN matrix can be effectively stable at ambient conditions. A low decomposition temperature of 600 K for N_8 chain is obtained, indicating that the h-BN matrix is an ideal confinement template for polymeric nitrogen N_8 chain. The dissociation barrier is 0.68 eV when polymer N_8 decomposed, which further confirms its kinetic stability at ambient conditions. The analyses of electronic density difference, band structure and DOS indicate that the charge transfer between host material and N_8 chain is the major responsibility for the stabilizing mechanism. Further analysis reveals that the charge transfer between N_8 chain and h-BN layer is much smaller than that of the previous works. Compared to the N_8@CNTs and N_8@BNNTs systems, the N_8@h-BN system has a smaller charge transfer due to the weaker host–guest interaction, which leads to a milder decomposition temperature. Finally, the weak host–guest interaction induces a red or blue shift of both the confined N_8 chain and h-BN matrix by the IR and Raman vibration analyses. These results provide an effective strategy for capturing and storing nitrogen-based HEDMs at ambient conditions and facilitating a more controlled energy release mechanism.

Conflicts of interest

There are no conflicts to declare.

Acknowledgements

References

1 X. Wang, Y. Wang, M. Miao, X. Zhong, J. Lv, T. Cui, J. Li, L. Chen, C. J. Pickard and Y. Ma, *Phys. Rev. Lett.*, 2012, **109**, 175502.

2 C. J. Pickard and R. J. Needs, *Phys. Rev. Lett.*, 2009, **102**, 125702.

3 Y. Li, X. Feng, H. Liu, J. Hao, S. A. T. Redfern, W. Lei, D. Liu and Y. Ma, *Nat. Commun.*, 2018, **9**, 722.

4 M. I. Eremets, M. Y. Popov, I. A. Trojan, V. N. Denisov, R. Boehler and R. J. Hemley, *J. Chem. Phys.*, 2004, **120**, 10618–10623.

5 D. Tomasino, M. Kim, J. Y. Smith and C.-S. Yoo, *Phys. Rev. Lett.*, 2014, **113**, 205502.

6 F. Zahariev, A. Hu, J. Hooper, F. Zhang and T. Woo, *Phys. Rev. B: Condens. Matter Mater. Phys.*, 2005, **72**, 214108.

7 D. Laniel, G. Geneste, G. Weck, M. Mezouar and P. Loubeyre, *Phys. Rev. Lett.*, 2019, **122**, 066001.

8 M. J. Greschner, M. Zhang, A. Majumdar, H. Liu, F. Peng, J. S. Tse and Y. Yao, *J. Phys. Chem. A*, 2016, **120**, 2920–2925.

9 S. V. Bondarchuk and B. F. Minaev, *Comput. Mater. Sci.*, 2017, **133**, 122–129.

10 F. J. Owens, *Comput. Theor. Chem.*, 2011, **966**, 137–139.

11 C. Mailhiot, L. H. Yang and A. K. McMahan, *Phys. Rev. B: Condens. Matter Mater. Phys.*, 1992, **46**, 14419–14435.

12 F. Zahariev, J. Hooper, S. Alavi, F. Zhang and T. K. Woo, *Phys. Rev. B: Condens. Matter Mater. Phys.*, 2007, **75**, 140101.

13 Y. Ma, A. R. Oganov, Z. Li, Y. Xie and J. Kotakoski, *Phys. Rev. Lett.*, 2009, **102**, 065501.

14 X. Wang, Z. He, Y. Ma, T. Cui, Z. Liu, B. Liu, J. Li and G. Zou, *J. Phys.: Condens. Matter*, 2007, **19**, 425226.

15 W. D. Mattson, D. Sanchez-Portal, S. Chiesa and R. M. Martin, *Phys. Rev. Lett.*, 2004, **93**, 125501.

16 B. Hirshberg, R. B. Gerber and A. I. Krylov, *Nat. Chem.*, 2014, **6**, 52–56.

17 H. Abou-Rachid, A. Hu, V. Timoshevskii, Y. Song and L. S. Lussier, *Phys. Rev. Lett.*, 2008, **100**, 196401.

18 W. Ji, V. Timoshevskii, H. Guo, H. Abou-Rachid and L.-S. Lussier, *Appl. Phys. Lett.*, 2009, **95**, 021904.

19 S. Liu, M. Yao, F. Ma, B. Liu, Z. Yao, R. Liu, T. Cui and B. Liu, *J. Phys. Chem. C*, 2016, **120**, 16412–16417.

20 V. Timoshevskii, W. Ji, H. Abou-Rachid, L.-S. Lussier and H. Guo, *Phys. Rev. B: Condens. Matter Mater. Phys.*, 2009, **80**, 115409.

21 F. Zheng, C. Wang and P. Zhang, *J. Comput. Theor. Nanosci.*, 2012, **9**, 1129–1133.

22 Z. Wu, M. Benchafia el, Z. Iqbal and X. Wang, *Angew. Chem.*, 2014, **126**, 12763–12767.

23 X.-L. Meng, N. Lun, Y.-X. Qi, H.-L. Zhu, F.-D. Han, L.-W. Yin, R.-H. Fan, Y.-J. Bai and J.-Q. Bi, *J. Solid State Chem.*, 2011, **184**, 859–862.

24 J. A. Perdigon-Melon, A. Auroux, C. Guimon and B. Bonnetot, *J. Solid State Chem.*, 2004, **177**, 609–615.

25 C. C. Tang, Y. Bando, X. X. Ding, S. R. Qi and D. Golberg, *J. Am. Chem. Soc.*, 2002, **124**, 14550.

26 G. Lian, X. Zhang, S. Zhang, D. Liu, D. Cui and Q. Wang, *Energy Environ. Sci.*, 2012, **5**, 7072–7080.

27 J. Li, J. Lin, X. Xu, X. Zhang, Y. Xue, J. Mi, Z. Mo, Y. Fan, L. Hu, X. Yang, J. Zhang, F. Meng, S. Yuan and C. Tang, *Nanotechnology*, 2013, **24**, 155603.

28 G. Kresse and J. Furthmuller, *Phys. Rev. B: Condens. Matter Mater. Phys.*, 1996, **54**, 11169–11186.

29 B. Hammer, *Phys. Rev. B: Condens. Matter Mater. Phys.*, 1999, **59**, 7413–7421.

30 J. P. Perdew, K. Burke and M. Ernzerhof, *Phys. Rev. Lett.*, 1996, **77**, 3865–3868.